

SEISMIC RESOLUTION AND FIELD DESIGN: SUCCESS AND FAILURE AT TABER, ALBERTA

GARY TAYLOR¹

ABSTRACT

Geophysical mapping is presented that suggests a genetic relationship may exist between a band of Glauconitic sandstone and the edge of a large Mississippian structure.

A seismic line of late 1970s vintage, covering a thick Glauconitic sandstone reservoir, was reshoot with a wider sweep, reduced geophone offsets and shorter arrays. These variations significantly improved the seismic visibility of the sandstone reservoir. However, they are also shown to significantly enhance the vulnerability of the signal to high-noise environments.

Such an environment is identified beneath a 163,000-volt transmission line with wooden poles, where ground roll from resonating poles, and not induced 60-Hz current, is shown to be the dominant noise system.

Examples are shown of the seismic signature for both structural and stratigraphically controlled reservoirs in the area.

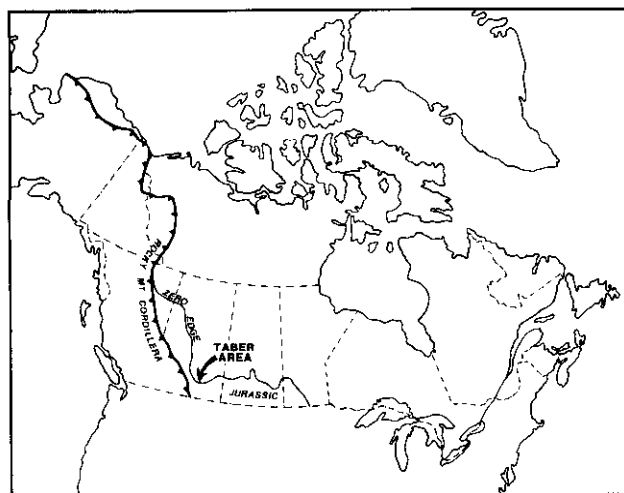


Fig. 1. Location of the Taber area: 100 km east of the Rocky Mountain Cordillera, 100 km north of the international boundary and the peak of the "Sweet Grass Arch", on the zero edge of the Jurassic. After Cook and Bally (1975).

GEOGRAPHY

CULTURAL GEOGRAPHY

The location of the study area is immediately north of the townsite of Taber on the plains of southwestern Alberta, Canada. It consists of a 19-km square, located about 100 km north of the border between Canada and the United States (Fig. 1).

The area is heavily cultured, with irrigation systems, powerlines, pipelines, railways, roadways and dwellings. As a result, most seismic data have been acquired with non-dynamite techniques: primarily Vibroseis*. The refinement of these techniques has been at the heart of a resource development effort that has been under way since 1975. As of the date of publication, this effort has established an area inventory of over $1.5 \times 10^6 \text{m}^3$ of recoverable oil.

PHYSICAL GEOGRAPHY

The area includes a large, S-shaped meander of the Oldman River system, with a valley cut of about 40 m (Fig. 2). This fluvial system, with its associated gravel lenses, causes combined elevation and drift corrections that can exceed 50 milliseconds. Refraction data from conventional Vibroseis* sources have not been able to resolve this static problem well enough for development work. For this reason, dynamite refraction data have often been acquired in tandem with Vibroseis* reflection profiles. Unfortunately, cultural problems severely curtail these supplementary dynamite surveys, so that, while they may reach the correct structural solution, it is with very poor consistency.

¹Canadian Superior Oil Ltd., 3 Calgary Place, Calgary, Alberta.

The author wishes to express his sincere gratitude to Graham Millington for his invaluable guidance throughout the preparation of this paper, as well as to Milan Hradsky, Michael Griffin and Ed Stacey for their work on the Taber area and for their helpful suggestions.

I also wish to thank the management and staff at Canadian Superior Oil Ltd. for releasing this material for publication. I am indebted to Susan Knuckey and the Canadian Superior drafting department for their work in preparing the manuscript.

*Registered trade and service mark of Continental Oil Company.

In summary, the geography of the Taber area is such that it is very difficult to acquire seismic data that are structurally reliable. Fortunately, there are two Cretaceous reflectors with enough structural stability to serve as datum surfaces for isochron maps: the Blackstone (Second White Specks marker) (Cook *et al.*, 1975) and the top of the Mannville group (McLean, 1981; Wall, 1981; Fingel, 1983). The more reliable of these has proved to be the Mannville, which was mapped from more than 600 boreholes to provide the required structural calibration for the seismic data (Fig. 2).

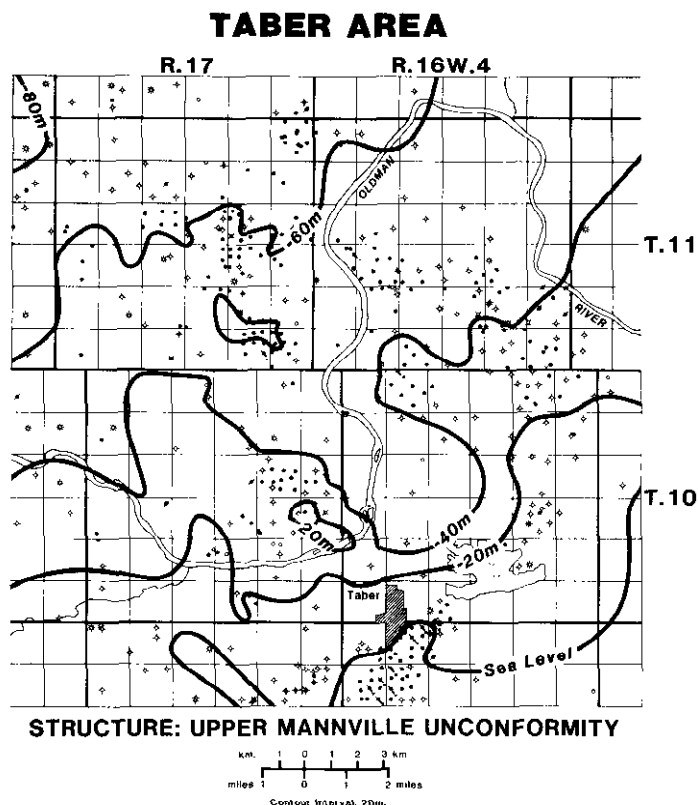


Fig. 2. Base map of the Taber area including Province of Alberta, Canada, Townships 10 and 11, Ranges 16 and 17, West of the 4th Meridian. The Old Man River cut is about 40 m deep \times 1 to 2 km wide. Structural contours are on the Upper Mannville unconformity, the datum marker for seismic maps to the Mississippian unconformity.

GEOLOGY

REGIONAL GEOLOGY - LOWER CRETACEOUS

The Taber area is located near the axis of a regional north-plunging anticline called "The Sweet Grass Arch" (Fig. 3). The western limb of the arch plunges steeply beneath the Rocky Mountain Cordillera, while the east limb dips gently into the Williston Basin (Wells, 1957). At the top of the Mannville, local dip is to the northwest and ranges from 2 to 25 m/km (Fig. 2).

Lower Cretaceous production comes from two members of the Lower Mannville Group: the "Glaucconitic Sandstone" (Fig. 4) and the "Taber Sandstone" (a northern equivalent of the "Cutbank" — Fig. 4). These are usually separated by the Ostracode limestone and the Ostracode (or Bantry) shale.

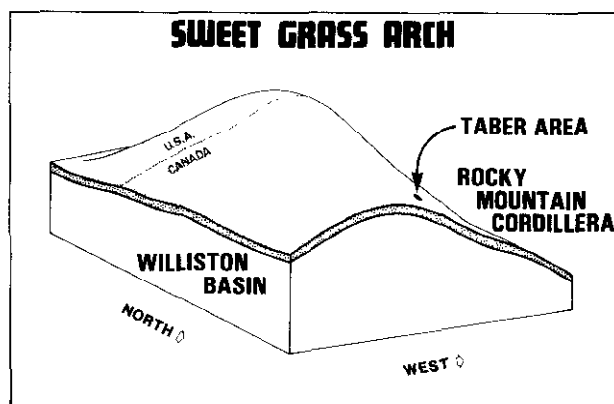


Fig. 3. Isometric drawing of the location of the Taber area in terms of the regional structural geology.

Both sandstones lie close to a large regional unconformity with Jurassic and Cretaceous clastics above and Mississippian carbonates beneath (Fig. 4). Jurassic shales cover this unconformity only in the southern part of the study area, where they are too thin to affect the seismic results. South of the study area, the Jurassic thickens and becomes an important part of the seismic profile.

STRUCTURAL GEOLOGY

Both structural and stratigraphic hydrocarbon traps are being exploited in the Taber area. Usually, Taber Sandstone reservoirs are structural and Glaucconitic Sandstone reservoirs are stratigraphic (Fig. 5).

Structural reservoirs occur in blanket Taber Sandstones when the overlying Ostracode Shale drapes into extreme lows on the Mississippian. Figure 6 shows the relative positions of Figures 7 and 8 (geologic cross Section A-A' and seismic profile a-a' respectively). The high, productive structure at the centre of Figure 8 is flanked on both sides by lows such as the one in the centre of Figure 7.

The low at the centre of Figure 7 was mapped across the study area from a composite data base of over 1200 km of seismic line and 600 boreholes. This study revealed five important attributes of this particular low, some of which may apply to other areas in southern Alberta.

- a) The edges of the low, which we will call the "Taber Low", are abrupt, with losses of up to 60 vertical metres across 400 m (Fig. 7).
- b) Relief on the Mississippian outside the Taber low is remarkably flat, so that many of the adjacent high areas are plateaus. Mississippian relief inside the Taber low is much more rugged.
- c) Seismic data quality, particularly at the Mississippian reflector, is usually poor inside the Taber low (Fig. 8).
- d) Seismic data quality over flat Mississippian surfaces outside the Taber low is nearly always very good (Fig. 8).

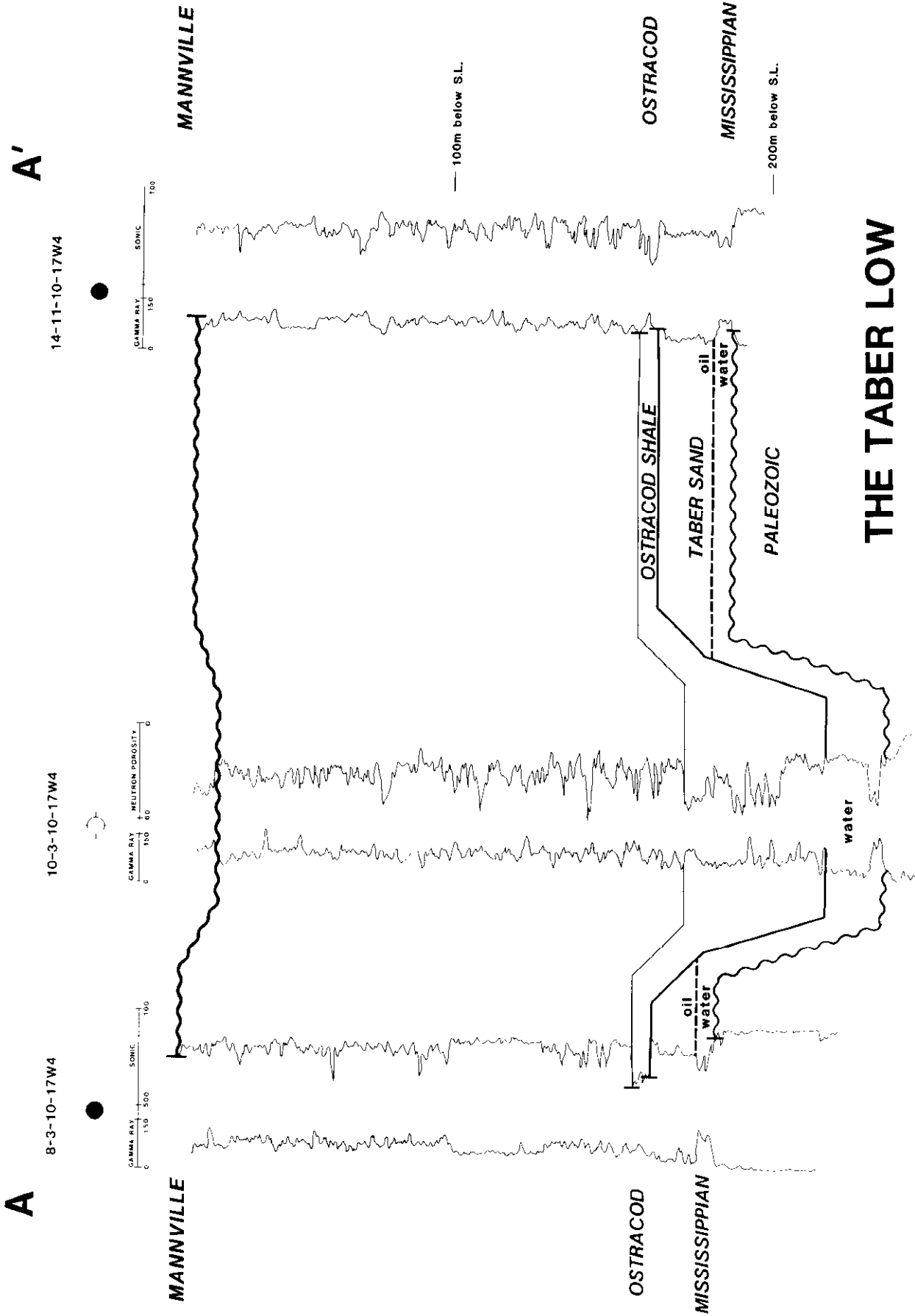


Fig. 7. Geologic cross section A-A' across an arm of the Taber Low (see Fig. 9).

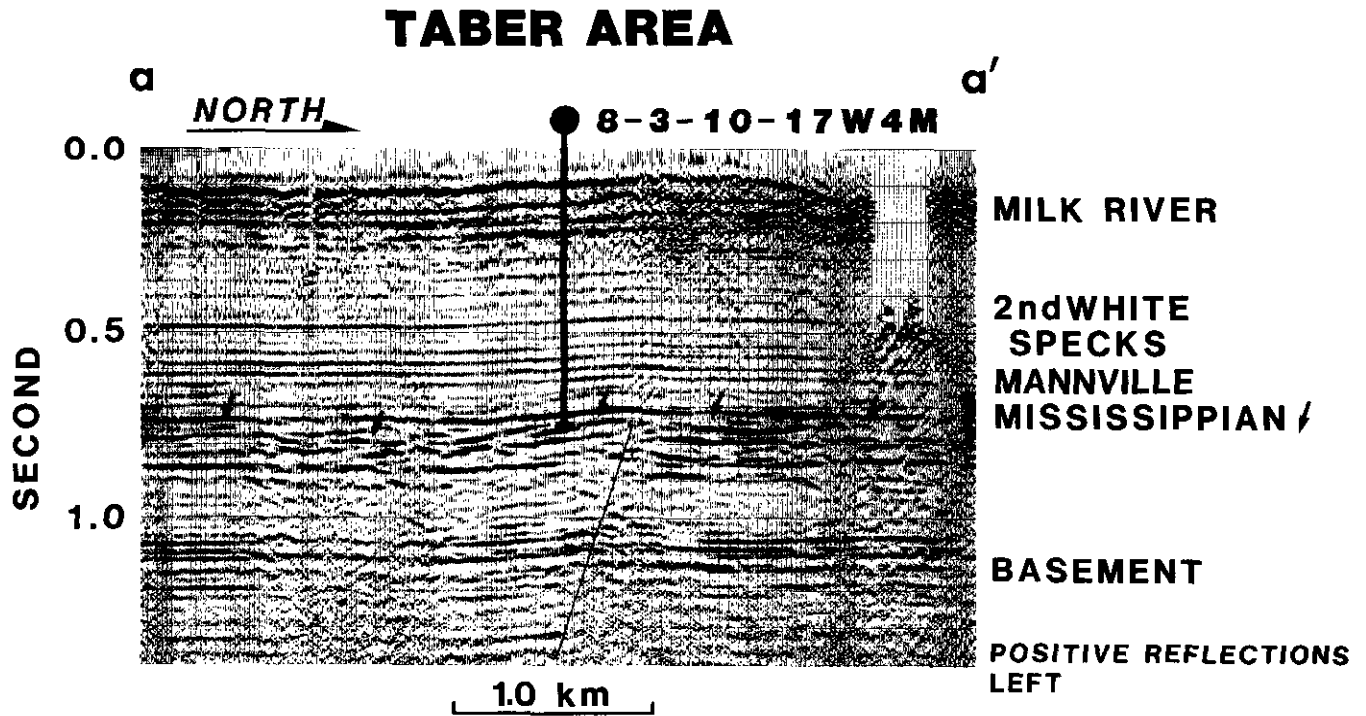


Fig. 8. Seismic profile a-a', probably straddling a plateau in the Taber Low (see Fig. 9).

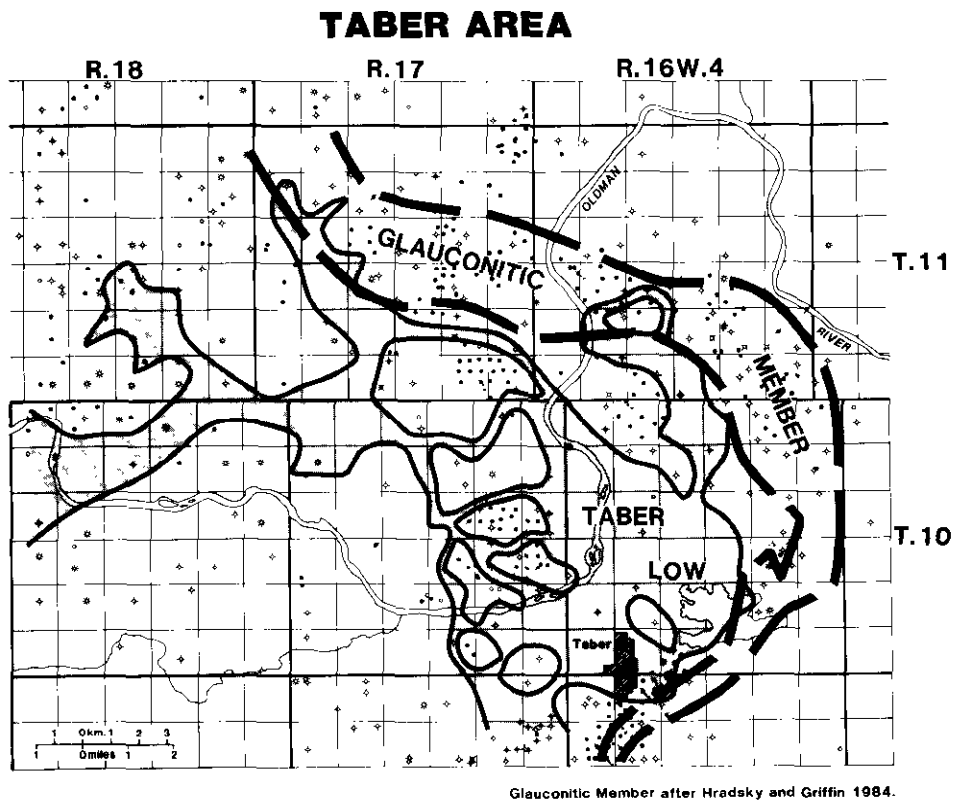


Fig. 9. The Taber Low, its approximate distribution across the Taber area and relative to the Glauconitic trend of Hradsky and Griffin (1984).

STRATIGRAPHIC GEOLOGY

For stratigraphic reservoirs to occur in Glauconitic sandstones, three conditions must be met:

- a) The sandstone must have good porosity.
- b) The porous sandstone must be embedded well enough into the overlying Mannville siltstones and shales to form a hydrocarbon trap (Fig. 5).
- c) The porous sandstone must be in hydrostatic communication with the Lower Mannville and Mississippian aquifer. For it is via this aquifer that hydrocarbon migration is thought to have taken place.

Cross section B-B' (Fig. 10) and seismic profile b-b' (Fig. 11) cover a stratigraphic reservoir in the northwest of the study area. The eastern borehole, 6M-14-11-17 W4M, is a dry hole because condition (a) above is not met. Notice the density contrast over the top of the Glauconitic zone in this dry hole, and compare it with the oil well in the centre. The density contrast in the centre well and the sonic contrast in the west well,

which are manifestations of good sandstone porosity, lead us to anticipate a seismic reflection from the top of the porous sandstone that is absent beneath the dry hole. This reflection is characteristic of all thick Glauconitic reservoir sands in the Taber area. In Figure 11 it appears beneath the two oil wells as the darkened peak at 0.690 s or 0.034 s above the Mississippian trough.

GEOPHYSICS

THE PROBLEM

Geologic cross section B-B' shows a vertical distance between the Mississippian and Glauconitic reflectors of roughly 55 m.

Cross section C-C' (Fig. 12) and seismic profile c-c' (Fig. 13) cover another stratigraphic reservoir in the east of the study area. They show a thick Glauconitic reservoir sandstone which is very similar to the one in Figure 10. Comparing cross sections B-B' and C-C', we find that the C-C' section is missing a significant gas cap, and roughly 15 m of section between the Missis-

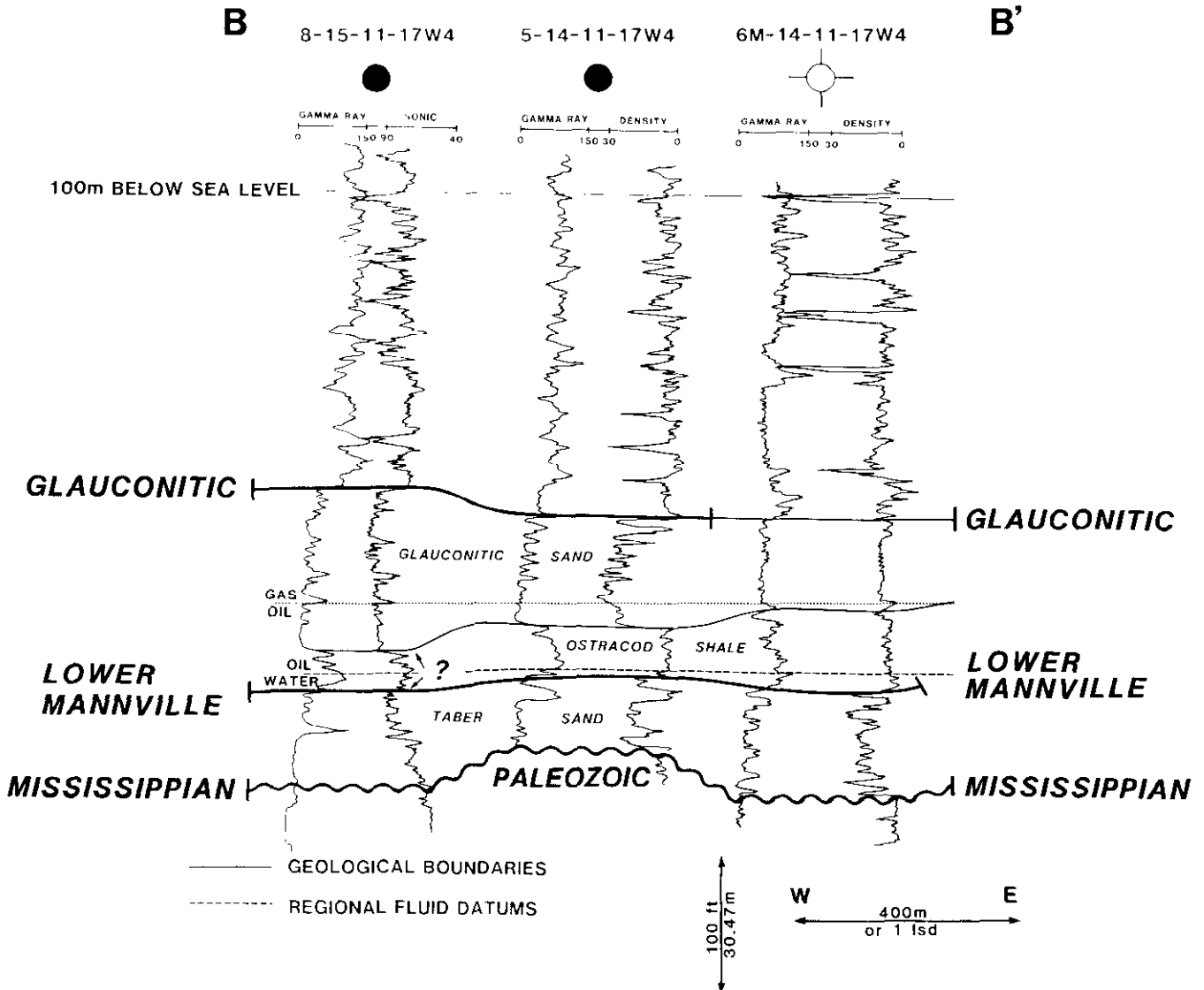


Fig. 10. Geologic cross section B-B' across a Glauconitic sandstone reservoir. Note the difference in density contrast across the Glauconitic from borehole 6M-14 to 5-14. Darkened formation boundaries indicate seismic reflectors.

sippian and the bottom of the reservoir sandstone.

In terms of the geophysics, the loss of the gas cap will result in a reduced density contrast at the top of the Glauconitic and a corresponding loss in the amplitude of the Glauconitic reflector. The loss of 15 m of Lower Mannville section between the Mississippian and the reservoir sandstone will result in a Glauconitic reflector

that is much closer to the Mississippian.

Figure 14 is a close-up of seismic profile c-c' at the thickest part of the reservoir sand. It shows that the Glauconitic reflector is so close to the Mississippian that it has been submerged into the overlying Lower Mannville peak, (cf. Figs. 11 and 14).

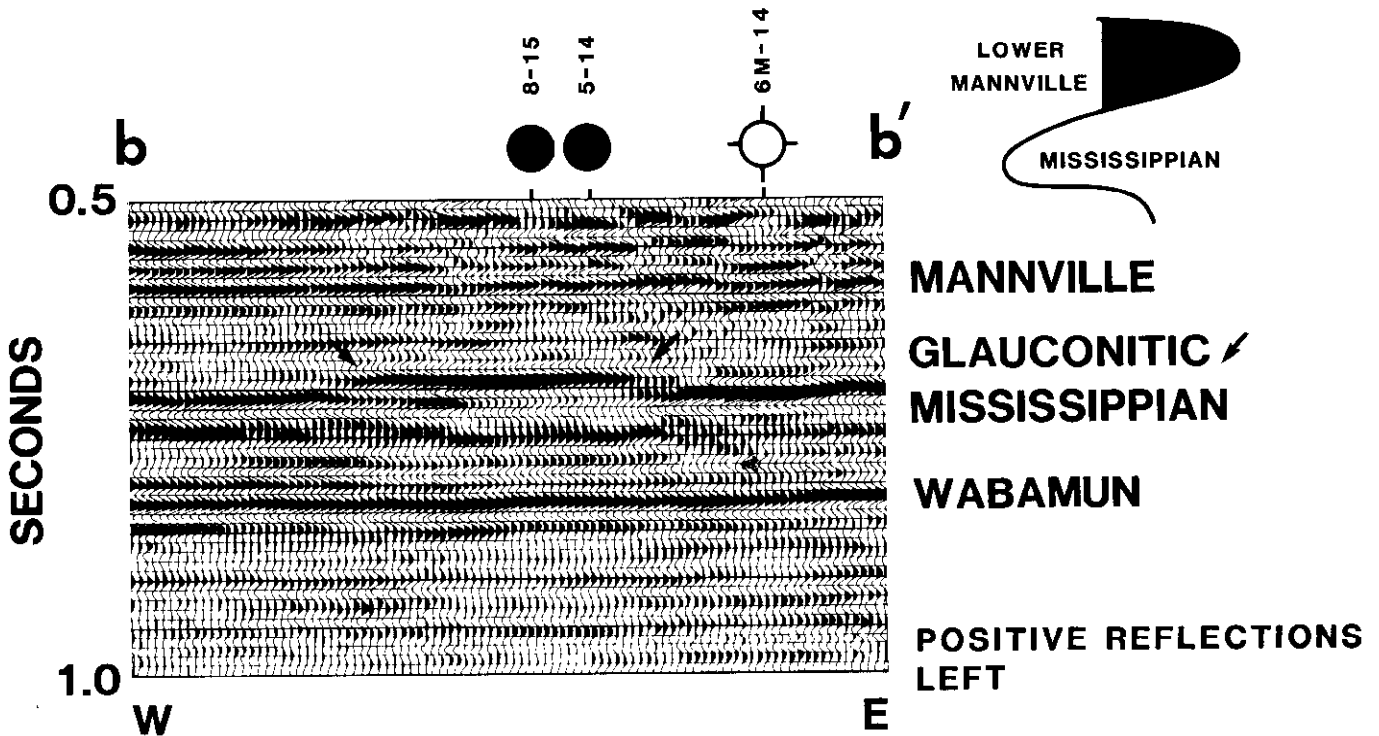


Fig. 11. Seismic profile b-b' along geologic cross section B-B'. Note the change in the Lower Mannville event from borehole 6M-14 to 5-14. Glauconitic arrows should point to the peak at 0.690 s and not the preceding trough.

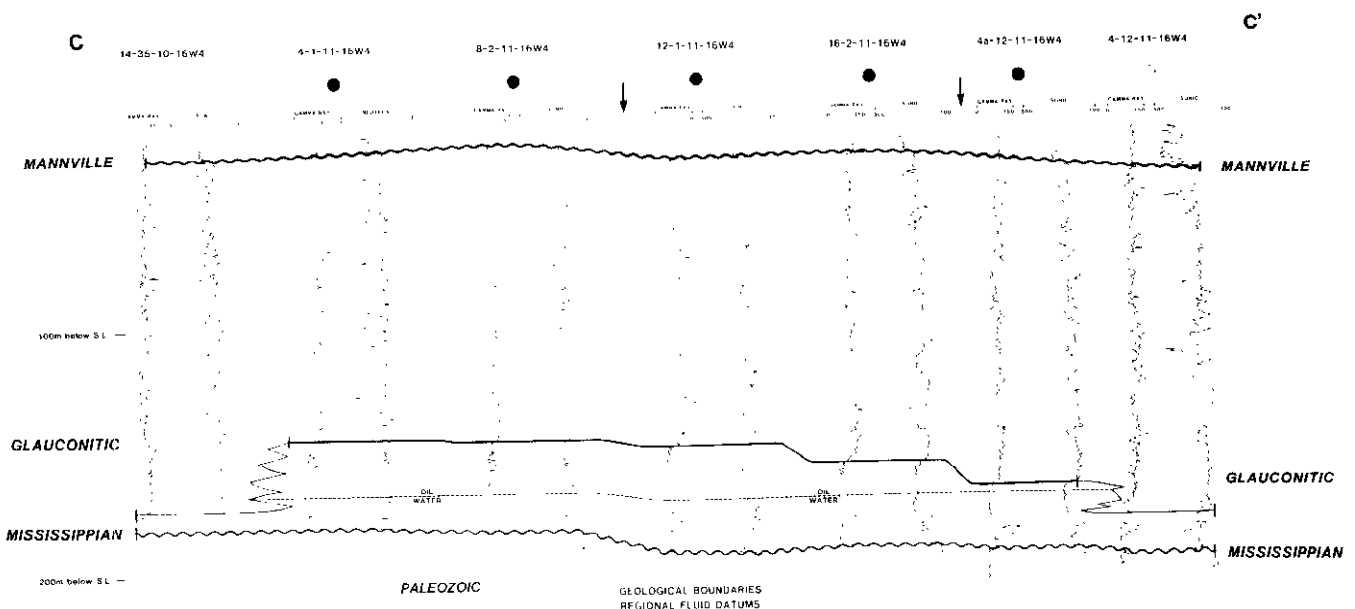


Fig. 12. Geologic cross section C-C' across a Glauconitic sandstone reservoir. This reservoir is closer to the Mississippian than B-B' and it has no gas cap. Darkened formation boundaries indicate seismic reflectors.

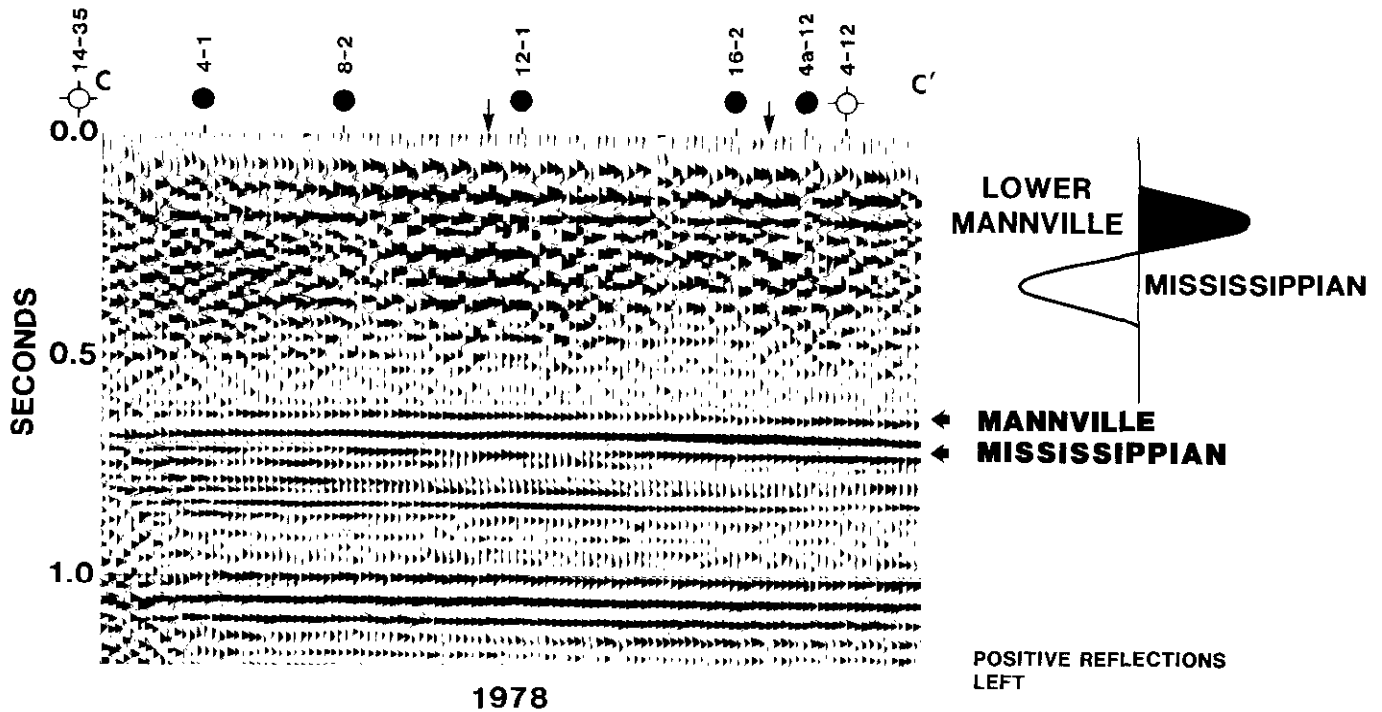


Fig. 13. Seismic profile c-c' along geologic cross section C-C'. Compare Lower Mannville peak with b-b'.

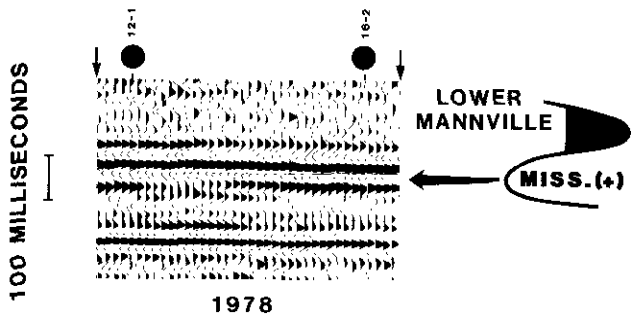


Fig. 14. Close-up of seismic profile c-c' (Fig. 13); window of interest between arrows at time zero.

THE SOLUTION

The solution, of course, requires the extension of the seismic bandwidth. Efforts to accomplish this through processing techniques proved unfruitful, largely because the vibrators used at the time of recording were unable to generate signal beyond 56 Hz.

We undertook to solve the problem in the field through the manipulation of three variables:

- a) Vibroseis* sweep
- b) geophone offset
- c) vibrator and geophone array lengths

a) *Vibroseis* Sweep*

The sweep rate was increased from 5.2 to 10.75 Hz/s and the width extended from a linear 56-14 Hz down-sweep to a linear 100-14 Hz down-sweep. Unfortunately, a strong multiple from the base of drift to the surface (Fig. 22) prevented us from extending the sweep below 14 Hz.

*Registered trade and service mark of Continental Oil Company.

b) *Geophone Offset*

An unfortunate side effect of normal move-out correction is signal stretching (Buchholtz, 1972; Dunkin *et al.*, 1973) but its effect on bandwidth can be quantified.

We begin with a sinusoidal time series of frequency f_a and offset $x = 0$. If C_0 is the number of sinusoidal oscillations across a particular time period $t_{0_2} - t_{0_1}$, then

$$f_a = \frac{C_0}{t_{0_2} - t_{0_1}}, (t_{0_2} > t_{0_1} > 0) \tag{1}$$

We next consider a sinusoidal time series of frequency f_a and offset $x \gg 0$. If C_x is the number of sinusoidal oscillations across a particular time period $t_{x_2} - t_{x_1}$, where

$$t_{x_1}^2 = t_{0_1}^2 + x^2/V_1^2 \tag{2}$$

$$t_{x_2}^2 = t_{0_2}^2 + x^2/V_2^2, (t_{x_2} > t_{x_1} > 0) \tag{3}$$

and V_2 and V_1 and stacking velocities at t_{0_2} and t_{0_1} respectively; then after normal move-out correction, the frequency f_b of the offset sinusoid is

$$f_b = \frac{C_x}{t_{0_2} - t_{0_1}} \tag{4}$$

Both the $x = 0$ and the $x \gg 0$ sinusoids began with frequency f_a before normal move-out, but $(t_{0_2} - t_{0_1}) > (t_{x_2} - t_{x_1})$, so that C_x will be less than C_0 by an amount proportional to the ratio of $(t_{x_2} - t_{x_1})$ to $(t_{0_2} - t_{0_1})$. Expressed as an equation, this will be

$$C_x = C_0 \left(\frac{t_{x_2} - t_{x_1}}{t_{0_2} - t_{0_1}} \right) \tag{5}$$

We define the loss of frequency due to normal move-out as

$$FI = \frac{fa - fb}{fa} \quad (6)$$

By simple substitution, this may be written as

$$FI = \left[\frac{Co}{(to_2 - to_1)} - \frac{Co (tx_2 - tx_1)}{(to_2 - to_1)^2} \right] \times \left[\frac{(to_2 - to_1)}{Co} \right] = 1 - \frac{tx_2 - tx_1}{to_2 - to_1} \quad (7)$$

The event of interest in the Taber area is from the Lower Mannville peak to the Mississippian trough (Fig. 14). Figure 15 shows frequency loss, FI, as a function of geophone offset, x , for this event. To keep FI below 25% it was necessary to restrict receiver spreads to less than 850 m. By extending the spreads to the point at which the zone of interest is muted, 1.1 km, some traces would have lost up to 40% of their original bandwidths.

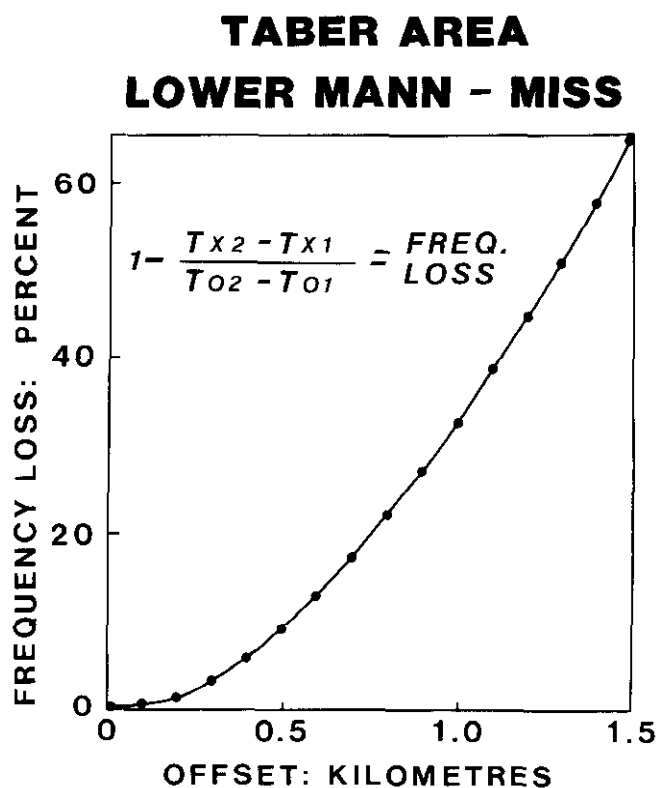


Fig. 15. Frequency loss due to normal move-out stretching as a function of geophone offset. Event 2 = Mississippian trough, event 1 = Lower Mannville peak. $V_2 = 3000$ m/s, $V_1 = 2925$ m/s, $to_2 = 0.715$ s, and $to_1 = 0.695$ s.

c) Vibrator and Geophone Array Length

Seismic profiles b-b' and c-c' were shot in the latter years of the last decade. Since that time a great deal of attention has been paid to the impact of field arrays and spatial sampling on temporal bandwidth (Berkhout, 1980).

Figure 16 is a frequency wavenumber display from a noise study in the Taber area. It shows that the wavenumber of a seismic reflection increases more or less linearly with increasing frequency. During the late 1970s most of the geophysical industry in Canada was using longer vibrator and geophone arrays. The response

of such an array is shown at the top of Figure 17. Clearly this array is very damaging to the higher frequency and wavenumber components of the signal. In 1983 experiments were done with shorter arrays. The response of one of these is shown at the top of Figure 18. The gentler slope will leave more of the high frequency and wavenumber components intact.

In summary, we undertook to improve the bandwidth of our CDP stacked seismic data to better resolve Glauconitic sandstone reservoirs. This was done by sweeping a wider range of frequencies, reducing our maximum geophone offset, and shortening the array lengths and spatial sampling intervals.

THE RESULTS

Figure 19 is an exact reshoot of seismic profile c-c' using the above field design. The expected improvement in bandwidth appears to have occurred, and a distinct event from the top of the Glauconitic sandstone is observable as it thickens from right to left (*cf.* Fig. 14).

However, not all of the results were this favourable. Another seismic profile, d-d', was shot in 1979 (Fig. 20) and then again in 1982 (Fig. 21) with the following field parameters:

Figure 20 (1979)

Sweep	56-14 down, linear, 8 s
Receivers	18 per group, 6.1 m apart
Vibrators	4 per sweep, 11.2 m apart
Moves	15 for 16 sweeps, 2.2 m per move
Drag Length	67 m
Near Receiver	201.2 m
Far Receiver	972.3 m
Group Interval	33.5 m

Figure 21 (1982)

Sweep	100-14 Hz down, linear, 8 s
Receivers	9 per group, 2.8 m apart
Vibrators	4 per sweep, 8.3 m apart
Moves	15 for 16 sweeps, 1.7 m per move
Drag Length	50 m
Near Receiver	125 m
Far Receiver	700 m
Group Interval	25 m

Hydrocarbon reservoirs in the south part of the study area where seismic profile d-d' was recorded are entirely structural in nature. Our primary objective in acquiring the data was to map the Mississippian structure. This objective demands that our first design priority should be recovering the Mississippian reflection. Extending the seismic bandwidth is less important in this case.

A comparison of Figures 20 and 21 makes it clear that in 1982 reflection recovery at all levels was inferior to the 1979 data. The loss of signal in the 1982 reshoot was severe enough that a noise study was undertaken to pursue its cause.

The noise study consisted of a simulated split spread with single receiver stations 2 m apart and offsets of

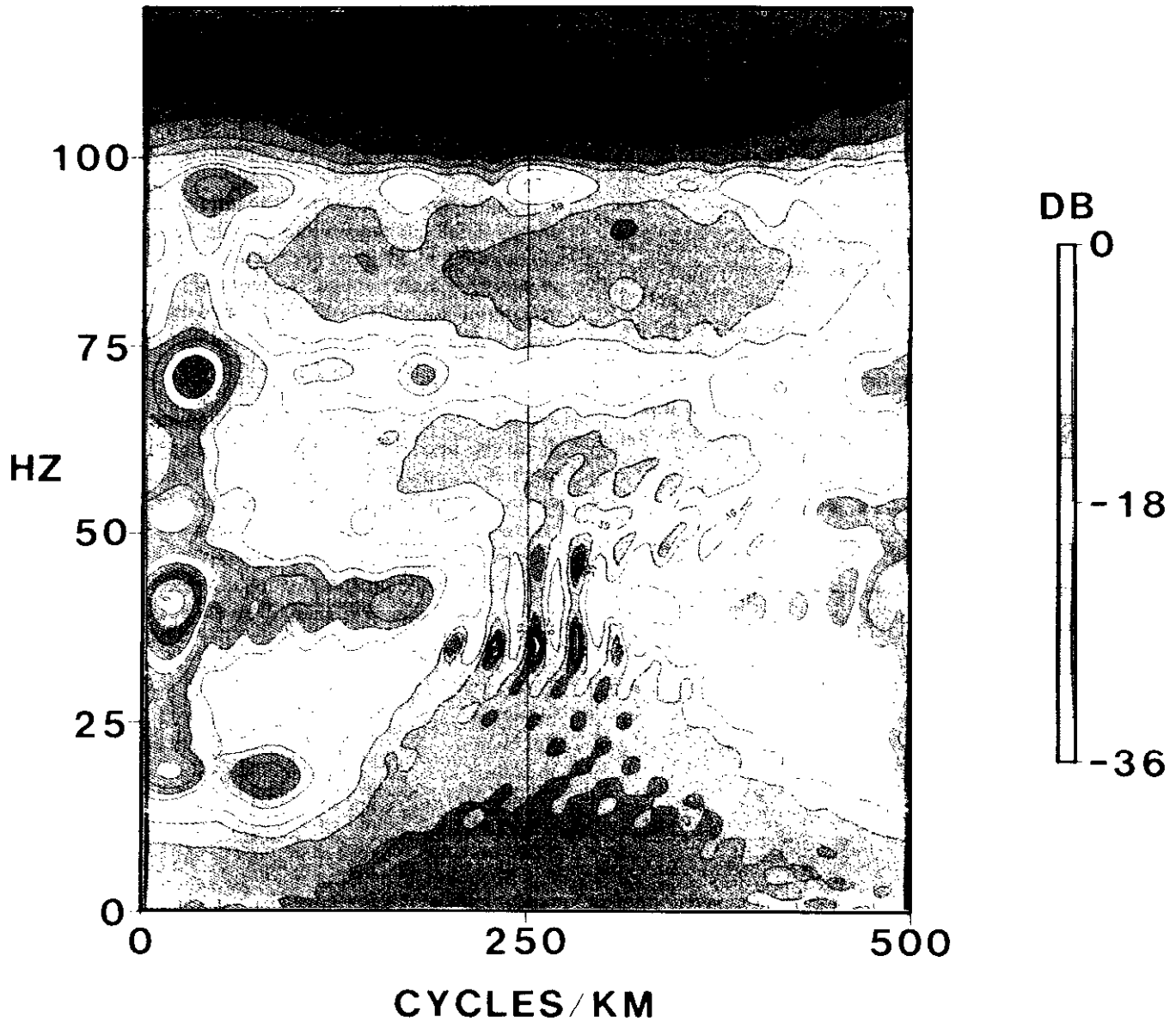


Fig. 16. Frequency-wavenumber display over a cosine tapered gate at $0 \leq t \leq 1.0$ s and $194 \leq x \leq 384$ m. Sweep was linear 100-14 Hz down, 8 s long from a single vibrator. Geophone groups were planted at one surface point per group, groups were 2 m apart. Spread was as shown in Figure 22.

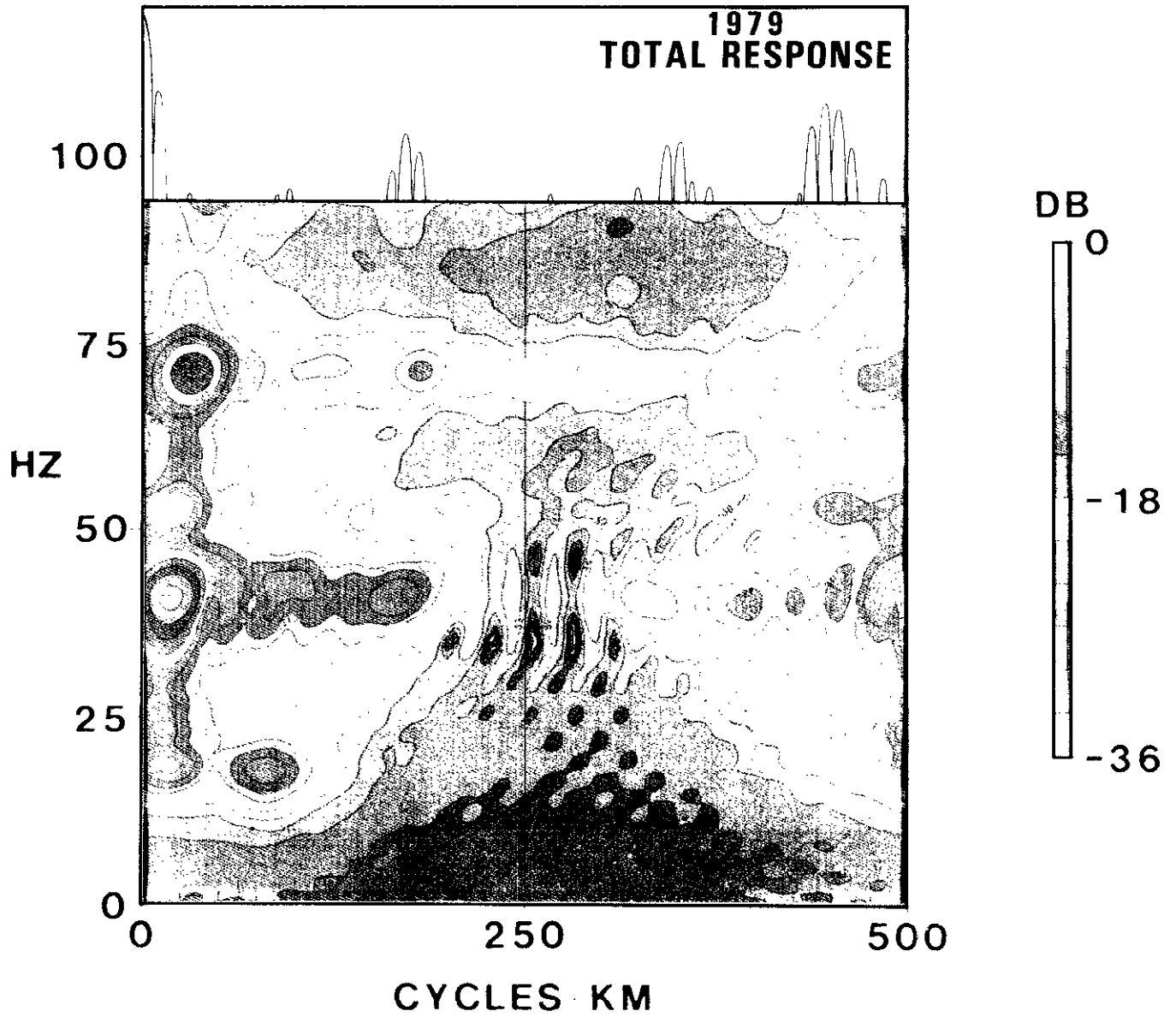


Fig. 17. Same as Figure 16. Inset at top is a total array response for: 4 vibrators, 11.2 m apart, drag 67 m, 15 moves, 16 sweeps, plus: 18 geophones, 5.9 m apart. Used 1979. Compare impact on higher frequency wavenumbers with Figure 18.

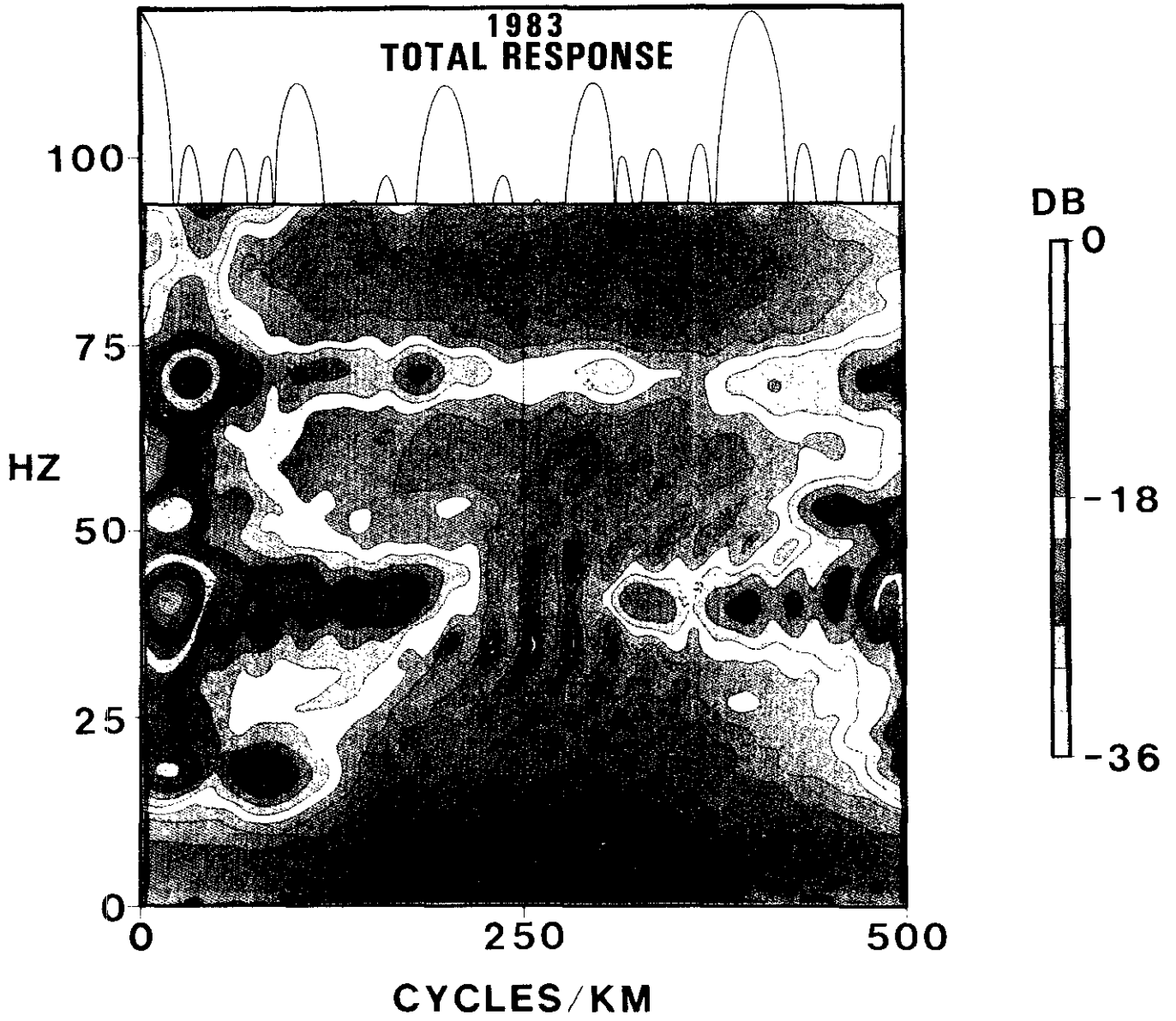


Fig. 18. Same as Figure 16. Inset at top is a total array response for: 4 vibrators, 10 m apart, drag 60 m, 3 moves, $4 \times 4 = 16$ sweeps, plus: 9 geophones 2.5 m apart. Used 1983.

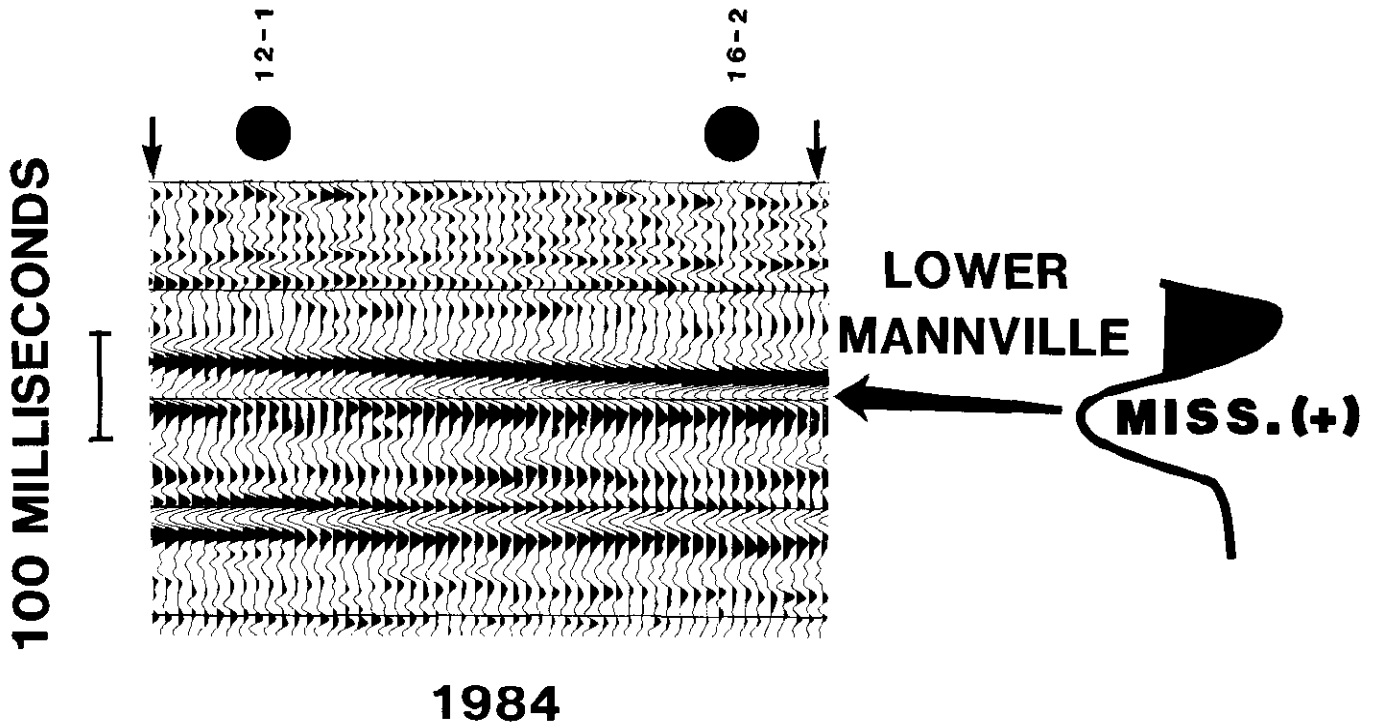


Fig. 19. Reshoot of seismic profile c-c', Figures 13 and 14, using wider sweeps, reduced geophone offsets and shorter arrays.

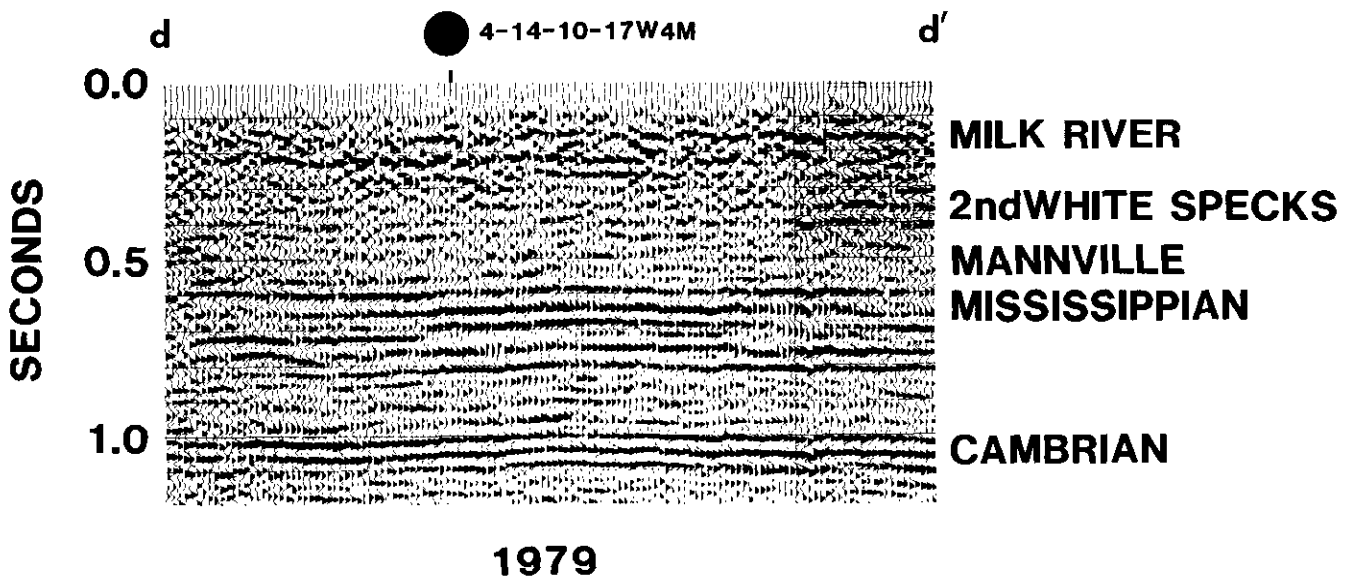


Fig. 20. Seismic profile d-d' as shot in 1979; compare with Figure 21.

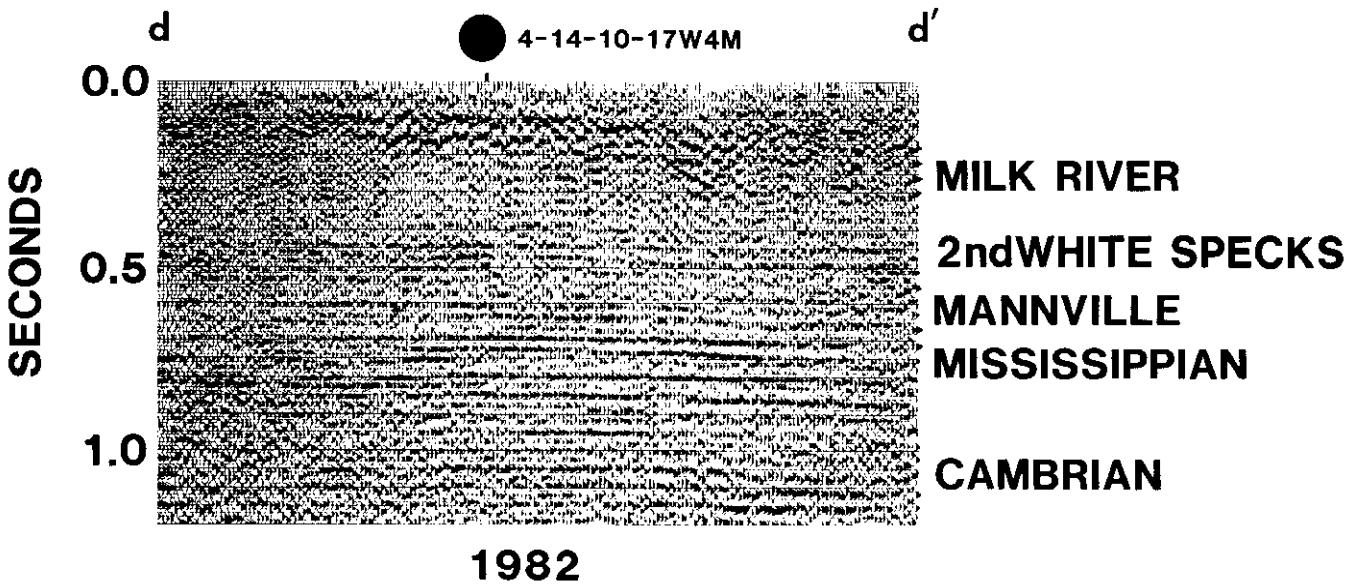


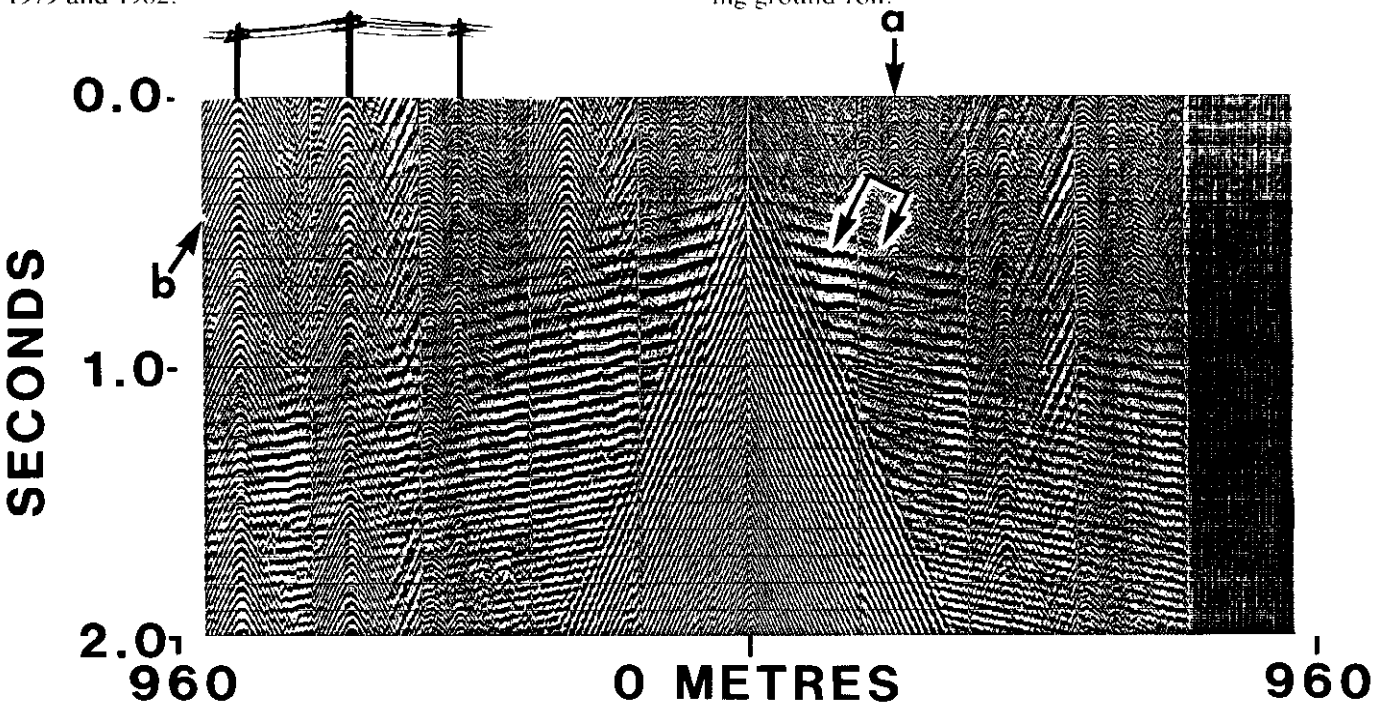
Fig. 21. Reshoot of seismic profile d-d' (Fig. 20), using wider sweeps, reduced geophone offsets and shorter arrays (see Fig. 22).

-960/0/+960. The spread was centred at a very abrupt boundary of the poor signal area, so that positive offsets were in good data and negative offsets were in poor data.

The noise study showed that the loss of signal was caused by a 163,000 volt power transmission line, but not by induced 60-Hz line noise. Both the 1979 and 1982 versions of the d-d' seismic profile were shot with notch filters in, and officials of the power utility company confirm that the line was built in 1963 and not between 1979 and 1982.

The noise study was done in winds estimated to have been under 10 km/h, but the large wooden poles of the transmission line were found to be mechanically resonating so much that it could be felt with the hand.

These resonating power poles set up the hyperbolic ground-roll pattern shown at the left of Figure 22. They are thought to have been the cause of the loss of signal experienced in the 1982 version of seismic profile d-d'. The earlier data employed long source and receiver arrays which were, by design, very effective in reducing ground-roll.



a: Surface to base of drift multiple.

b: Ground-roll pattern from resonating power poles.

PASS # 1

Fig. 22. Taber Area noise study with point receivers and sources, shows a surface to base of drift multiple and a hyperbolic noise pattern from a large power pole. These power poles are thought to have caused the poor reflection recovery seen in Figure 21 (1982).

Figure 23 was recorded by using 3 vibrators 10 m apart with peak piston force at 25%/50%/25%; Figure 22 was recorded with a single vibrator at 100% of peak piston force. A comparison shows that the power-pole noise pattern is severely reduced in Figure 23. There are three possible reasons for this reduction.

1. The vibrator array of Figure 23 is a 100-cycle/km spatial notch filter. This is the dominant wavenumber of ground-roll in the Taber area.
2. The assigned peak piston force in the vibrator is not exact and the energy of the 3-vibrator array may have greater than that of the single vibrator.
3. The resonance of the power pole fluctuated from hour to hour and was not necessarily the same for both records.

ity than the data processor for spatial filter design. This is because he or she may use individual sources or receivers as filter points, whereas the data processor is often confined to composite sums of multiple sources and/or groups of geophones. The long source and geophone arrays of the late seventies were often appropriate for the largely structural nature of the reservoirs being drained at that time, but for stratigraphic work they tend to filter away a very important component of the signal — the higher frequencies and wavenumbers. Field parameter design for structural or stratigraphic work is no more, or less, than spatial filter design. The same rules and principles applicable to the design of temporal filters apply to that of spatial filters, and to the

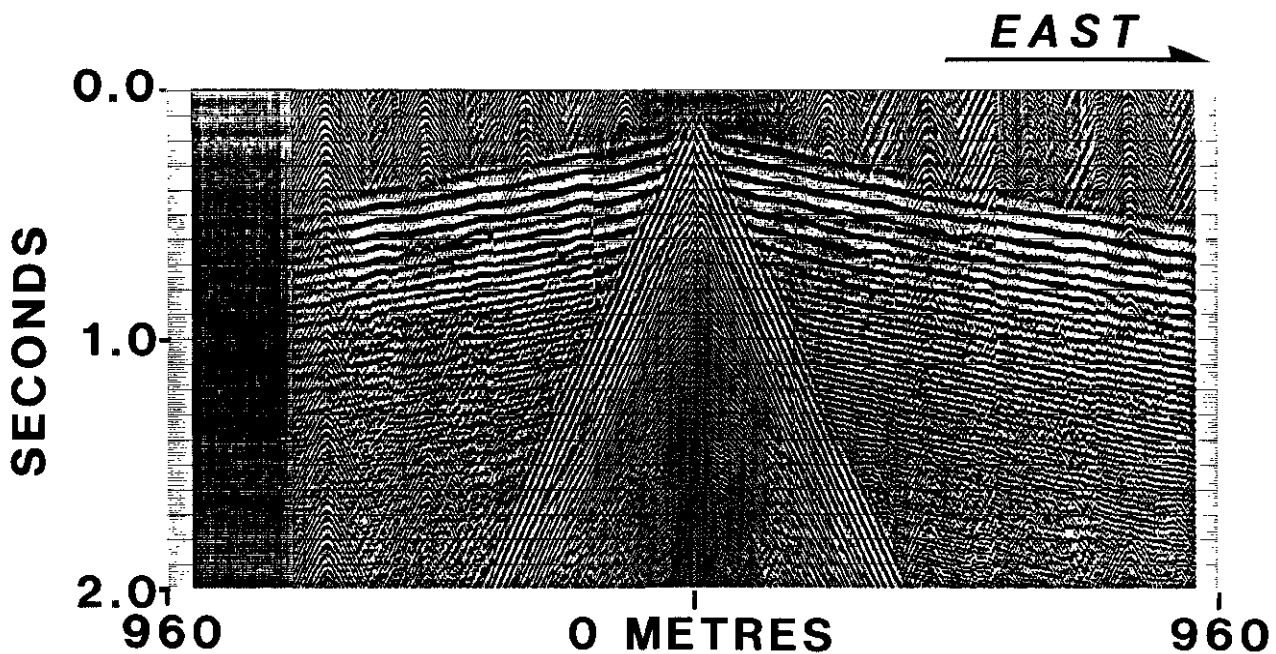


Fig. 23. Taber area noise study: 3 vibrators, 10 m apart at 25%/50%/25% of peak piston force. Same coverage as above (Fig. 22).

The noise study showed that the 1982 version of seismic profile d-d' was probably affected by ground-roll from resonating transmission poles with a resulting loss in signal-to-noise ratio. It also demonstrated a possibility that the 1979 data were less affected because of the very powerful spatial filters used at that time through vibrator and geophone arrays.

CONCLUSIONS

At present the field designer has much more flexibil-

design of appropriate field parameters.

An important trend in the Glauconitic Member of the Lower Mannville extends across the Taber area from northwest to southeast. This trend appears to follow an abrupt Mississippian structural edge such that it always remains on its high side. The correlation of this Glauconitic trend with such a Mississippian edge may imply a genetic relationship between the edge and the distribution of the overlying sediments.

REFERENCES

- Berkhout, A.J. 1980, Seismic Migration: Amsterdam, Elsevier, p. 291-296.
- Bucholtz, H. 1972, A note on signal distortion due to dynamic (NMO) corrections: *Geophysical Prospecting*, v. 20, p. 395-402.
- Cook, T.D. and Bally, A.W. 1975, *Stratigraphic Atlas of North and Central America*, Shell Oil Company: Princeton University Press, Princeton, New Jersey, p. 203-215.
- Dunkin, J.W. and Levin, F.K. 1973, Effect of normal moveout on a seismic pulse: *Geophysics*, v. 38, p. 635-642.
- Finger, K.L. 1983, Observations on the Lower Cretaceous Ostracode zone of Alberta: *Bulletin of Canadian Petroleum Geology*, v. 31, p. 326-337.
- Hopkins, J.C. *et al.* 1982, Morphology of channels and channel-sand bodies in the Glauconitic sandstone member (Upper Mannville), Little Bow area, Alberta: *Bulletin of Canadian Petroleum Geology*, v. 30, p. 274-285.
- Hradsky, M. and Griffin, M. 1984, Sandstone body geometry, reservoir quality and hydrocarbon trapping mechanisms in Lower Cretaceous Mannville Group, Taber/Turin area, southern Alberta: *Canadian Society of Petroleum Geologists, Memoir 9*, p. 401-411.
- McLean, J.R. 1981, Lithostratigraphy of the Lower Cretaceous coal bearing sequence, Foothills of Alberta: *Geological Survey of Canada, Paper 80-29*, 31p.
- Wall, J.M. 1981, The Early Cretaceous Moosebar Sea in Alberta: *Bulletin of Canadian Petroleum Geology*, v. 29, p. 334-377.
- Wells, G.C. 1957, The Sweetgrass Arch area — southern Alberta: *Alberta Society of Petroleum Geologists, 7th Annual Field Conference Guidebook*, September 1957, p. 27-45.